Multihazard Interaction Effects on the Performance of Low-Rise Wood-Frame Housing in Hurricane-Prone Regions

Vipin U. Unnikrishnan, Ph.D., A.M.ASCE[1]; and Michele Barbato, Ph.D., P.E., M.ASCE[2]

Abstract: Hurricanes represent multihazard events that include wind, windborne debris, storm surge, and rainfall hazards. Conventional risk analysis does not consider the interaction between these multiple hazards and treats each risk source as statistically independent of other hazards. In this paper, the effects of multihazard interaction on the performance of low-rise wood-frame residential buildings subject to hurricane hazard are investigated using the performance-based hurricane engineering (PBHE) framework. The use of different hazard-modeling techniques and vulnerability analysis approaches is examined. A new, consistent terminology to classify different hazard-modeling techniques is also proposed. A case study consisting of a realistic building in an actual residential development in Charleston, South Carolina, is presented to investigate the effects of hazard interaction in the different phases of the PBHE framework. Three different hazard-modeling techniques (based on different amounts of available statistical information) and two vulnerability analysis approaches (global vulnerability and assembly-based vulnerability) are considered, for a total of six combinations of loss analysis results for each location. It is concluded that the use of different hazard models and vulnerability approaches can significantly affect the final results of a loss analysis. **DOI: 10.1061/(ASCE)ST.1943-541X.0001797.**

Author keywords: Multihazard analysis; Performance-based engineering; Hurricane engineering; Loss analysis; Residential buildings; Wood-frame housing; Wind effects.

Introduction

Structures located in coastal regions at tropical and subtropical latitudes are at high risk of suffering severe damages and losses from wind, windborne debris, surge, and rainfall hazards due to tropical storms and hurricanes. As the population tends to concentrate in coastal regions and the number of residential buildings in hurricane-prone areas continues to rise, the societal vulnerability to hurricanes is increasing, with the prospect of even higher damages and losses in the future (Li and Ellingwood 2006). Early studies on hurricane hazard assessment and mitigation focused on the damage and loss from individual hazards such as wind alone or storm surge alone. Powell and Houston (1995) proposed a real-time damage assessment model based on a damage function relating various meteorological variables to the percentage of damage to the buildings. Thomalla et al. (2002) built a storm surge and inundation model for the risk assessment of residential buildings. Discrete damage states were identified and assigned on the basis of inundation and component damage of the building. Li and Ellingwood (2006) developed a probabilistic risk assessment methodology to assess the performance and reliability of low-rise light-frame wood residential constructions subject to hurricane wind hazard.

Conventional multihazard risk analyses, such as those used by FEMA's Hazards United States Multi-Hazards (*HAZUS-MH*) software, consider each risk source as statistically independent of other hazards and do not consider the interaction among multiple hazards (Pang et al. 2014). Dao and van de Lindt (2012) presented a methodology, which was based on the combination of existing wind tunnel data and a rainwater intrusion model, for estimating the probability of rainwater intrusion into each room of typical wood-frame structures subjected to hurricanes. Li et al. (2012) introduced a loss-based approach for design of light-frame wood buildings in areas prone to more than one natural hazard. Correlation of hazards was not considered in these studies.

Phan et al. (2007) proposed a methodology for creating site-specific joint distributions of combined hurricane wind and surge using full-track hurricanes to compute the wind speed and the Sea, Lake, and Overland Surge from Hurricanes (SLOSH) model to estimate surge heights (Jelesnianski et al. 1992). Lin and Vanmarcke (2010) developed an integrated vulnerability model that explicitly accounts for the correlation between windborne debris damage and wind pressure damage, obtained by coupling a pressure damage model derived from the component-based model of the Florida Public Hurricane Loss Model (Gurley et al. 2005) and the windborne debris risk model developed by Lin and Vanmarcke (2008). Needham and Keim (2014) examined the relationship between storm surge heights and tropical cyclone wind speeds at 3-h increments preceding landfall and observed that storm surge magnitudes correlate better with prelandfall wind speeds than with wind speeds at landfall. Pei et al. (2014) developed joint hazard maps of combined hurricane wind and surge for Charleston, South Carolina. The surface wind speeds and surge heights from individual hurricanes were respectively computed using Georgiou's wind field model (Georgiou 1985) and the SLOSH model (Jelesnianski et al. 1992).

Vickery et al. (2006) presented an overview of the damage and loss models used in *HAZUS-MH* and proposed wind-windborne

[1]Principal Research Consultant, Impact Forecasting LLC., Aon Benfield, Whitefield, Bangalore, Karnataka 560066, India. E-mail: vipin.unnithan.u@aon.com

[2]Associate Professor, Dept. of Civil and Environmental Engineering, Louisiana State Univ., Baton Rouge, LA 70803 (corresponding author). E-mail: mbarbato@lsu.edu

Note. This manuscript was submitted on June 8, 2016; approved on January 13, 2017; published online on March 29, 2017. Discussion period open until August 29, 2017; separate discussions must be submitted for individual papers. This paper is part of the ***Journal of Structural Engineering***, © ASCE, ISSN 0733-9445.

debris damage states for residential buildings. Womble et al. (2006) developed a joint hurricane wind–surge damage scale based on a loss-consistent approach using *HAZUS-MH*'s damage and loss functions and U.S. Army Corps of Engineers (USACE) flood depth-loss functions (USACE 2000) for the assessment of damage from combined wind and flood events. van de Lindt and Taggart (2009) proposed a methodology for performance-based design and loss analysis of wood buildings subjected to flood hazard using an assembly-based vulnerability model. The methodology involved calculation of the damage suffered by each building component and the corresponding cost of repair or replacement.

Li et al. (2012) conducted a risk assessment analysis for residential buildings that estimated the combined losses from hurricane wind, storm surge, and rainwater intrusion. They considered the correlation between wind and surge by implementing a hurricane-induced surge model through regression analysis of historical data. Pita et al. (2012) presented an approach to assess the interior building damage caused by hurricanes by simulating the co-occurrence of wind, rain, and envelope damage. The vertical free-falling rainfall rate was estimated as a function of the storm's radius and maximum wind speed and was converted into an unobstructed impinging rainfall rate using a semiempirical framework proposed by Straube and Burnett (2000). Barbato et al. (2013) developed the Performance-Based Hurricane Engineering (PBHE) framework and applied it to risk assessment of residential buildings subjected to wind and windborne debris impact. They also investigated the effect of interaction between the sources of wind and windborne debris impact hazards on the expected annual loss (EAL) assessment. Unnikrishnan and Barbato (2015, 2016b) used the PBHE framework for risk assessment of nonengineered buildings subject to combined wind, windborne debris, flood, and rainfall hazards. Correlation of these hazards was considered only implicitly, by modeling rainfall and flood hazards as functions of hurricane wind speed. A global vulnerability analysis approach was adopted. The annual probabilities of loss exceedance and the EAL of the target building were computed for different individual hazards and their interactions. They also emphasized the need to consider the multihazard nature of hurricane events for accurate probabilistic loss analysis.

This paper investigates the effects of interactions among multiple hazard sources and the modeling approaches that can be employed in different phases of the PBHE framework to incorporate them. To the authors' knowledge, the present study is the first of its kind to explicitly quantify the effects of multihazard interaction and different modeling approaches in the PBHE framework. Different typologies of hazard models available in the literature are identified and investigated based on their level of complexity and amount of information required to use them. Similarly, different vulnerability-modeling techniques used in performance-based risk assessment are identified and described in the PBHE framework. A consistent terminology is also proposed to classify the different hazard models and vulnerability analysis approaches available in the literature. A realistic case study is presented to illustrate these interaction effects on the risk assessment for a typical house of an actual residential development located in Charleston, South Carolina. The EALs computed using different hazard models and vulnerability-modeling approaches are compared for three different neighborhoods in Charleston, which correspond to different multiple hazard scenarios and are selected to investigate the effects of different hazard and vulnerability models on the loss analysis under different hazard scenarios.

Summary of PBHE Framework

The PBHE framework proposed in Barbato et al. (2013) disaggregates the performance assessment procedure for structures subject to hurricane hazard into elementary phases that are carried out in sequence. The structural risk in the PBHE framework is expressed by the probabilistic description of a decision variable, DV, which is defined as a measurable quantity that describes the cost and/or benefit for owner, users, and/or society resulting from the structure under consideration. The fundamental relation for the PBHE framework is given by

$$G(DV) = \iiiii G(DV|DM) \cdot f(DM|EDP) \cdot f(EDP|IM,IP,SP) \cdot f(IP|IM,SP) \cdot f(IM) \cdot f(SP) \cdot dDM \cdot dEDP \cdot dIP \cdot dIM \cdot dSP \quad (1)$$

where $G(\bullet)$ = complementary cumulative distribution function and $G(\bullet|\bullet)$ = conditional complementary cumulative distribution function; $f(\bullet)$ = probability density function and $f(\bullet|\bullet)$ = conditional probability density function; IM = vector of intensity measures (characterizing the environmental hazard); SP = vector of structural parameters (describing the relevant properties of the structural system and nonenvironmental actions); IP = vector of interaction parameters (describing the interaction between the environment and the structure); EDP = engineering demand parameters (describing the structural response for the performance evaluation); and DM = damage measures (describing the physical damage to the structure). By means of Eq. (1), the performance assessment is disaggregated into the following tasks: (1) hazard analysis, (2) structural characterization, (3) interaction analysis, (4) structural analysis, (5) damage analysis, and (6) loss analysis. Additional details on the general PBHE framework and its specialization to nonengineered structures can be found elsewhere (Barbato et al. 2013; Unnikrishnan 2015; Unnikrishnan and Barbato 2016a, b).

Multihazard Characterization of Hurricane Events

Multihazard interactions can occur at two levels (Zaghi et al. 2016): (1) through the nature of the hazards (also called Level-I interactions), when the interactions among multiple hazards are independent of the presence of physical components; and (2) through the effects of the hazards (also called Level-II interactions), when the interactions among multiple hazards take place through "site effects, impacts on physical components, network and system disruptions, and social and economic consequences" (Zaghi et al. 2016). Level-I multihazard interactions among different natural and man-made hazards can be classified into the following three modalities (Barbato et al. 2013; Gill and Malamud 2014): (1) independent hazards, i.e., hazards that are not correlated in nature and/or that derive from different sources/extreme events, which can be acting at different times or at the same time; (2) interacting hazards, i.e., hazards that increase or decrease the probability of occurrence and/or the intensity of other hazards; and (3) hazard chains or cascading hazards, when one hazardous event (primary hazard) triggers one or more different hazards (secondary hazard). In the case of hurricane events, four different hazards are acting at the same time: (1) strong winds, (2) windborne debris, (3) storm surge, and (4) heavy rain. The wind hazard is always interacting with all other hazards by increasing their intensity when the wind speed increases, whereas windborne debris and storm surge are practically independent of each other. According to the definition provided previously, the four co-occurring hazards considered in this study are not cascading hazards by themselves but could be the triggering effects for other hazards (e.g., heavy rain triggering landslides), possibly producing chain hazards. The investigation of potential chain hazards triggered by hurricane events is beyond the scope of this paper.

Consideration of Level-II hazard interactions is also crucial for the performance assessment of structures subject to hurricane hazards. One of the most important aspects to be accounted for is the fact that the effects of some hazards can modify (usually amplify) the effects of other hazards on a given structure. In this paper, the terms "chain hazard effects" and "cascading hazard effects" are used to distinguish this situation from that of hazards' triggering other hazards (i.e., hazard chains or cascading hazards). For hurricane events, cascading hazard effects can be significant; for example, windborne debris and storm surge can produce hazard chain effects (by producing breaches in the building envelope) with the wind and rainfall hazard (Unnikrishnan and Barbato 2016a).

In this section, the multihazard interaction modalities and available modeling approaches in each of the different analysis phases of the PBHE framework are discussed in detail. A consistent terminology is also proposed to identify different approaches used in the literature to model interactions among the different hazards characterizing a hurricane event. Particular attention is given to the different interaction modeling in the hazard and loss analysis phases because the range of modeling options available for these two analysis phases is wider than for other analysis phases; thus the selection of different hazard or vulnerability models can most affect the performance assessment of low-rise residential buildings subject to hurricane hazard.

Interaction in the Hazard Analysis Phase

The hazard analysis phase of the PBHE framework is used to model Level-I interactions for independent and interacting hazards. For independent hazards, independent models are adopted to statistically describe the corresponding intensity measures. For interacting hazards, different models can be adopted to describe the correlation between different hazard intensity measures. These models can be classified in terms of modeling complexity and required statistical information.

In terms of modeling complexity, three approaches of increasing complexity and computational cost can be used to determine the statistical description of the intensity measures of interest. In the lowest-complexity approach, the statistics of the different intensity measures (e.g., 3-s gust wind velocity, V, and/or storm surge height, ζ) are directly obtained from existing records at the building site (Boon et al. 1978; Batts et al. 1980; Li and Ellingwood 2006). This approach is referred to as "direct statistics approach" hereafter. In the intermediate-complexity approach, the statistics of the different intensity measures are obtained indirectly based on the site-specific statistics of fundamental hurricane parameters such as storm maximum wind speed, V_{max}, storm radius of maximum wind, R_{max}, and storm central pressure deficit, Δp (Batts et al. 1980; Vickery and Twisdale 1995). This approach is referred to as "indirect statistics approach" hereafter. Finally, the highest level of complexity directly models the possible full tracks of hurricanes from initiation over the ocean to final dissipation and uses these tracks to obtain the intensity measure statistics of interest at the building site (Vickery et al. 2000). This approach is referred to as "full track approach" hereafter.

In terms of amount of statistical information required to fully describe the statistical models for the intensity measures, three modeling approaches can be identified for use in the PBHE framework: (1) those based on a limited set of primary intensity measures described through their marginal probability distributions, referred to as "primary distribution models" (PDMs); (2) those based on a complete set of intensity measures, each described by its marginal probability distributions, referred to as "multiple distribution models" (MDMs); and (3) those based on the joint probability distributions of the complete set of intensity measures, referred to as "joint distribution models" (JDMs). Any of the three complexity approaches can be used in conjunction with any of the three statistical information levels; however, higher-complexity models are often paired with higher levels of statistical information (Vickery et al. 2000).

Primary Distribution Models or PDMs

The PDMs consider the statistical distribution of one or a few intensity measures, usually used to describe a single hazard (referred to as primary-intensity measures hereafter), and describe all other derived intensity measures (for the same or other hazards) as functions of the primary intensity measures. These functions are usually developed using regression analysis of historical data (in the form of explicit functions; e.g., Conner et al. 1957) and/or simulations (in which case the relations between primary- and derived-intensity measures are implicit; e.g., Tuleya et al. 2007; Irish et al. 2008). The earlier PDMs used a direct statistics approach and, for example, predicted surge height as a function of storm central pressure deficit as $\zeta = A \cdot \Delta p^B$, where A and B = regression coefficients; and Δp = primary intensity measure (Conner et al. 1957). With the advent of efficient computers, numerical hydrodynamic models (based on more advanced indirect statistics or full-track approaches) were developed to forecast hurricane surge heights based on hurricane parameters, storm track, and local topographic and bathymetric data. Some of these models include SLOSH (Jelesnianski et al. 1992), the Advanced Circulation Model (Luettich et al. 1992), the Coastal Marine Environment Prediction System (Pietrafesa et al. 2002), and the Finite Volume Coastal Ocean Model (Chen et al. 2003). A common characteristic of PDMs is that derived intensity measures are usually highly correlated with primary intensity measures and thus often overestimate the actual correlation between different intensity measures.

Multiple Distribution Models or MDMs

MDMs use marginal distributions of all pertinent intensity measures obtained from historical data and/or simulations. The correlations between different intensity measures are neglected. The direct statistics approach can be used to obtain the statistical characteristics of hurricane wind speed by fitting hurricane wind speed records, such as those provided by the National Institute of Standards and Technology (NIST), to appropriate probability distribution functions (Barbato et al. 2013). The wind speed records provided by NIST contain data sets of simulated 1-min hurricane wind speeds at 10 m above the ground in open terrain near the coastline for locations ranging from Milepost 150 (near Port Isabel, Texas) to mile post 2850 (near Portland, Maine), spaced at 50-nm (92,600-m) intervals. Similarly, the statistical characteristics of surge and rainfall can be directly derived for example from the National Weather Service (NWS) Cooperative Observer Program (NWS 2016) and the National Oceanic and Atmospheric Administration (NOAA) National Centers for Environmental Information database (NOAA 2016), respectively. The indirect statistics or full track approach can also be employed using appropriate models and neglecting the correlation between different intensity measures.

Joint Distribution Models or JDMs

JDMs can be developed from historical records and/or numerical simulations, for example joint wind-surge (Phan et al. 2007; Pei et al. 2014) and joint wind-rain models (Rosowsky et al. 2016). Also, in this case the direct statistics, indirect statistics, or full track approach can be used to obtain the marginal distribution and the correlation between the intensity measures. For the direct statistics approach, in addition to the records for each intensity measure, information is needed regarding the contemporaneity of the data

relative to different quantities. For the indirect statistics approach, site-specific statistics of the basic hurricane parameters can be used in conjunction with appropriate numerical models to obtain wind, surge, and rainfall at any location. Similarly, for the full track approach the joint statistics of the intensity measures can be obtained by modeling the full track of hurricanes and combining that with surge (SLOSH, Advanced Circulation Model, etc.) and rainfall (Tuleya et al. 2007; *HAZUS-MH*) numerical models. Once the marginal distributions of the pertinent intensity measures and their correlations are obtained, different techniques are available in the literature to generate the joint probability distribution of the intensity measures—for example, the Chow-Liu tree (Chow and Liu 1968), the Nataf transformation (Der Kiureghian and Liu 1986), and the copula-based approach (Nelsen 2007).

Interaction due to Cascading Hazard Effects

The Level-II interaction of hazards may occur in the form of cascading hazard effects, when the effects of some hazards modify sequentially the effects of other hazards on a structure. For example, the actions on a structure due to windborne debris can damage the building envelope—for example, by damaging brittle components such as glass windows and doors. This damage to the building envelope can increase the structure's vulnerability to strong winds by transforming it from an enclosed building to a partially enclosed one, for which the internal pressure coefficients are significantly higher (Li and Ellingwood 2006; ASCE 2010). The increase in the internal pressure coefficients can further amplify damage to the building envelope and initiate a chain reaction until the building collapses. The study of hazard chain effects requires modeling structural system configuration and properties as functions of the level of structural damage caused by the different hazards. In particular, the presence of hazard chain effects implies that structural parameters can change as a consequence of damage measures exceeding specified thresholds. Barbato et al. (2013) and Unnikrishnan and Barbato (2016a) investigated hazard chain effects due to the interaction between windborne debris and wind hazards on residential building loss analysis. These studies highlighted the importance of cascading hazard effects for accurate hurricane risk assessment of low-rise residential buildings.

Interaction in the Loss Analysis Phase

Level-II multihazard interactions can occur in the loss analysis phase, and their effects on risk assessment and design depend on the type of vulnerability analysis being performed. In fact, losses are produced by different hazards, which tend to affect simultaneously different components of the structural system of interest. Two kinds of vulnerability analyses are commonly considered in the existing literature and are illustrated here (1) global vulnerability and (2) assembly-based vulnerability.

Global Vulnerability Analysis

Global vulnerability analysis is a widely used methodology in seismic risk assessment of structures (FEMA 2007; Nielson and DesRoches 2007). In this approach, buildings are classified into different (discrete) damage states based on damage to individual components and the structure's global response. Unnikrishnan and Barbato (2015) used the global damage-state model proposed by Womble et al. (2006) for performance-based hurricane risk assessment of residential structures subject to multiple hazards. The use of this approach in hurricane loss analysis requires knowledge of loss statistics associated with each global damage state, which can be obtained from insurance claims, when available, and/or numerical simulations (e.g., from assembly-based vulnerability analysis). Global vulnerability analysis is computationally very efficient because total loss is estimated based only on the global damage state of the building. However, its accuracy can be significantly affected by imprecision in damage state classification and scarcity of information in determining loss statistics for each damage state.

Assembly-Based Vulnerability Analysis

Assembly-based vulnerability analysis was originally proposed by Porter et al. (2001) to calculate building loss due to seismic hazard. It involves dividing the entire building into components based on specific building details. Building-specific damage and loss estimation procedures are developed at the component level. Component response and fragility curves are used to evaluate the damage level for each individual component. It is assumed that the total loss in a building is equal to the sum of repair and/or replacement costs of the individual components damaged during the hazard event. Assembly-based vulnerability analysis was later adopted in the risk assessment of residential buildings subjected to hurricanes (Gurley et al. 2006; Li et al. 2012; *HAZUS-MH*; Unnikrishnan and Barbato 2016a). One of the main features of this approach is that the loss due to each component produced by each hazard can be easily identified and accounted for in the risk assessment procedure. Hence, the approach allows estimation of the effect of each component damage on total loss and it simplifies the choice of appropriate risk mitigation techniques. However, obtaining a complete inventory of all components and their repair/replacement costs is a complex task. In addition, the greater computational effort associated with assembly-based vulnerability analysis makes its application cumbersome when compared with global vulnerability analysis.

Interactions in Other Intermediate Analysis Phases

In addition to the interactions in the hazard and loss analysis phases, which have predominant effects in risk analysis for low-rise wood-frame residential buildings, hazard interactions can be identified in any intermediate analysis phase of the PBHE framework. This section briefly illustrates some of these possible interactions, which may be important for other applications of the PBHE framework.

Structural Characterization Phase

The structural parameters of a system can affect Level-II interactions among different hazards. For example, internal and external pressure coefficients are correlated (Beste and Cermak 1997), and this correlation can affect wind-windborne debris cascading hazard effects. Building elevation is another structural parameter that influences hazard interaction because increasing it can reduce the risk associated with flooding due to storm surge; however, it may also increase the wind pressure acting on the building.

Interaction Analysis Phase

In the interaction analysis phase, hazard interaction mainly depends on the models used to obtain the interaction parameters and on the correlation between different parameters used in them. For example, the correlations between debris flight time and debris flight distance or between debris flight distances in the along-wind and across-wind directions can significantly affect Level-I interactions between wind and windborne debris hazards (Barbato et al. 2013; Unnikrishnan and Barbato 2016a). Similarly, the correlation between wind pressures acting on different components of the building can also affect the breaching of the building envelope and thus the Level-II interaction between wind and windborne debris hazards.

Structural Analysis Phase

In the structural analysis phase, Level-II hazard interactions can depend on the correlation between the material constitutive parameters used to model the structural system, which affect structural

response to different hazards. However, because the structural analysis phase is not explicitly for non/pre-engineered buildings such as those considered here (Unnikrishnan and Barbato 2016a), the interaction in the structural analysis phase is not considered in this study.

Damage Analysis Phase

The resistance of both structural and nonstructural components in a building can sometimes be positively correlated because of common construction materials, fabrication, and construction practices (Mori 2005). For example, if a house is well built, often all elements are of good quality and vice versa. However, the quality of construction can significantly vary between different components and even between different parts of the same component, resulting in negligible or negative correlation between the strength of different portions of the same structure. The actual correlation between different structural and nonstructural components is usually difficult to quantify because of a lack of data.

This correlation, or its lack, can also affect the hazard interaction and the results of a vulnerability analysis. Thus, when using the PBHE framework, the capacity correlation between different components should be included in the vulnerability analysis whenever reliable data are available to estimate it. However, when the data are insufficient, a more prudent approach is to assume that the capacities of different components are uncorrelated, as assumed hereinafter.

Application Example

This study presents as an example a hurricane risk analysis for a single-family one-story wood-frame house subject to wind, windborne debris, surge, and rainfall hazards. The analysis is performed using the multilayer Monte Carlo simulation implementation of the PBHE framework (Barbato et al. 2013; Unnikrishnan and Barbato 2016a, b). The effects of hazard interaction at the hazard and loss analysis levels on the risk analysis performed using the PBHE framework are investigated. An actual residential development located in South of Broad, Charleston, South Carolina, is considered in this study (Fig. 1). To compare the effects of the interaction in the hazard analysis phase, three locations were selected in Charleston: Roper Hospital, South of Broad, and French Quarter (Fig. 2). They were chosen because they respectively correspond to three different hazard scenarios: predominant wind losses, predominant surge losses, and comparable losses from wind and surge. The elevation above mean sea level of the base of the building at the three location is 2.99, 1.95, and 2.11 m, respectively.

To accurately estimate loss annual probability of exceedance (APE), 100,000 samples were used for all results. Six sets of results are presented here for each location: (1) PDM in conjunction with global vulnerability analysis, (2) PDM in conjunction with assembly-based vulnerability analysis, (3) MDM in conjunction with global vulnerability analysis, (4) MDM in conjunction with assembly-based vulnerability analysis, (5) JDM in conjunction with global vulnerability analysis, and (6) JDM in conjunction with assembly-based vulnerability analysis. It is assumed that the building is fully repaired after each hurricane event.

Benchmark Structure and Structural Characterization

The simple residential building used by van de Lindt and Taggart (2009) is considered here as a benchmark structure (the location of which in the residential development is identified by a red circle in Fig. 1). The value of the target structure is taken as $180,000, and the content value is assumed equal to $90,000. Fig. 3 is a plan view of the target residential building, including its (deterministic)

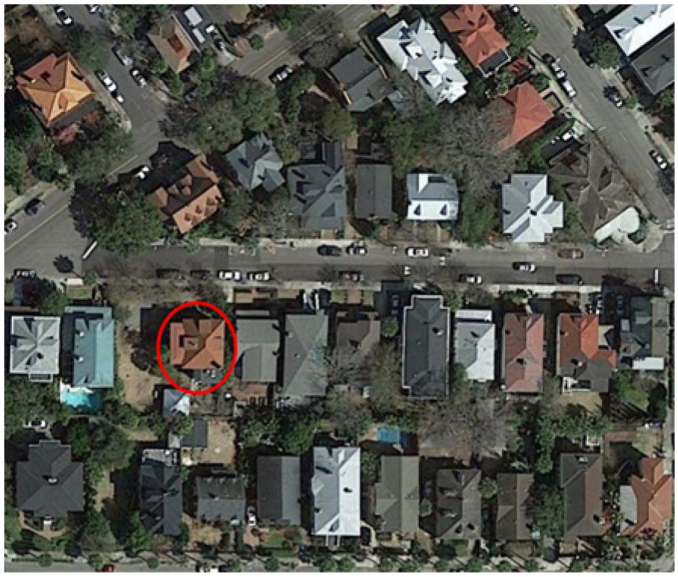

Fig. 1. Plan view of the residential development (map data © 2016 Google)

Fig. 2. Selected locations in Charleston (map data © 2016 Google)

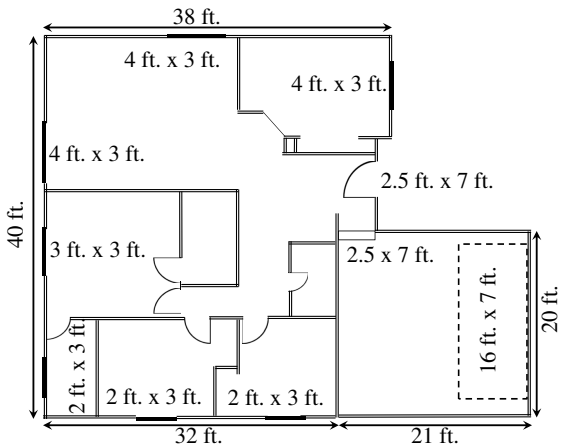

Fig. 3. Plan view of the benchmark building (1 ft = 0.305 m)

geometric parameters. Detailed building dimensional information can be found in Taggart (2009).

The base structure is characterized by (1) roof cover made of asphalt shingles, (2) nailing pattern 8d C6/12 for the roof sheathing—8-mm-diameter smooth shank nails with 15.2-cm (6-in.) spacing at the center and 30.5-cm (12-in.) spacing at the edge, (3) unprotected windows and doors, and (4) wooden walls. Walls and windows are considered to be debris-impact vulnerable. The wind pressure exposure factor K_h is assumed as normally distributed with a mean value of 0.71 and a coefficient of variation (COV) of 0.19. The topographic factor is modeled as a deterministic quantity with value $K_{zt} = 1$. The statistical characterization of the external and internal pressure coefficients can be found in Unnikrishnan and Barbato (2016a).

Hazard Analysis

Three hazard models are considered: PDM, MDM, and JDM. In this study, a direct statistics approach is used to obtain the statistics of the different intensity measures. However, most of the data used to obtain these statistics were taken from Pei et al. (2014), in which a full-track approach was used to derive data on wind speed and storm surge height. In all models, the number of hurricanes per year is simulated using a Poisson occurrence model, with an annual hurricane occurrence rate $\nu_{\text{hurricane}} = 0.42$, which was also obtained from the data provided by Pei et al. (2014). The roof covers of all houses in the residential development are considered potential windborne debris sources. Because the debris generation model employed by the Florida Public Hurricane Loss Model (Gurley et al. 2005) is adopted here for all three models, the number of generated debris, n_{debris}, is not discussed further because it is always treated as a derived intensity measure that depends on 3-s wind speed and the position of buildings in the residential development relative to the benchmark building.

Hazard Analysis Based on PDM

The following quantities are selected as primary intensity measures: 3-s wind speed at 10 m above the ground, V, maximum hurricane wind speed, $V_{\max}$, radius of maximum wind, $R_{\max}$, and central pressure deficit, Δp. The derived intensity measures are surge height, ζ, and impinging rainfall rate, IRR. Hurricane wind speed variability is described using a Weibull distribution (Unnikrishnan and Barbato 2016a), the parameters of which are fitted through maximum likelihood estimation of the hurricane wind speed records obtained from Pei et al. (2014) for the three locations. The radius of maximum wind is assumed to follow a lognormal distribution with mean equal to 24 km and COV equal to 0.28, and the central pressure deficit is assumed to follow a Weibull distribution with mean equal to 44.38 mbar and COV equal to 0.46 (Huang et al. 2001).

Storm surge height distribution is obtained using a hurricane-induced surge model proposed by Irish et al. (2008). This model is based on the regression analysis of numerically simulated storm surge data obtained from a coupled hurricane vortex–planetary boundary layer model (Thompson and Cardone 1996) to estimate sustained near-surface winds throughout the storm. The surge height is computed as

$$\sqrt{\hat{\zeta}} = \begin{bmatrix} \sqrt{\hat{R}_{\max}} & 1 \end{bmatrix} \cdot C(S_0) \cdot \begin{bmatrix} \Delta\hat{p}^2 \\ \Delta\hat{p} \\ 1 \end{bmatrix} \tag{2}$$

where $\hat{\zeta} = \zeta \cdot g/V'^2$; $\hat{R}_{\max} = R_{\max} \cdot g/V'^2$; $\Delta\hat{p} = \Delta p/p_{\text{atm}}$; V' = 1-min wind speed = $0.79V$; $g = 9.81$ m/s^2 = gravity constant; p_{atm} = atmospheric pressure; S_0 = ocean slope (assumed to be constant and equal to 1:5000); and $C(S_0) = \begin{pmatrix} -1.078 \times 10^{-1} & 3.996 \times 10^{-2} & 4.444 \times 10^{-4} \\ 3.974 \times 10^{0} & -1.093 \times 10^{0} & -1.653 \times 10^{-1} \end{pmatrix} = 2 \times 3$ curve fitting coefficient matrix.

This model does not capture the effects of local topography and provides the same surge height for any given wind speed at all three locations considered. The correlation coefficient between wind speed and surge height obtained through direct simulation using this model varies between 0.93 and 0.95.

The impinging rainfall rate, IRR, is calculated using the rainfall hazard model proposed in the Florida Public Hurricane Loss Model (Pita et al. 2012) as a linear function of 3-s gust speed and is given by

$$IRR = a \cdot V - b \tag{3}$$

where a and b = dimensional regression coefficients, with values of 0.128 cm · s/m and 0.65 cm, respectively, for Charleston determined by using historical hurricane data obtained from the Iowa Environment Mesonet database (IEM 2001).

Hazard Analysis Based on MDM

The following quantities are selected as intensity measures: 3-s wind speed at 10 m above the ground, V, surge height, ζ, and impinging rainfall rate, IRR. The marginal distribution of V is obtained as for the PDM by fitting a Weibull distribution to the data provided by Pei et al. (2014). The marginal distributions of ζ and IRR are obtained by fitting the empirical cumulative density function of the surge data provided by Pei et al. (2014) and the historical rainfall data from the Iowa Environment Mesonet database (IEM 2001), respectively. Fig. 4 shows the hazard curves in terms of APE for each intensity measure based on the MDM (assuming no correlation between the different intensity measures).

Hazard Analysis Based on JDM

The following quantities are selected as intensity measures: 3-s wind speed at 10 m above the ground, V; surge height, ζ; and impinging rainfall rate, IRR. The intensity measures are described by the same marginal distributions obtained for the MDM. In this study, a copula-based approach with a Gaussian copula is used to generate the joint probability distribution of the intensity measures. The efficiency investigation of different copulas in modeling the dependence structure of the variables, albeit important, is out of the scope of this study. A Gaussian copula function is generated for V, ζ, and IRR, based on the marginal distributions and the correlation coefficients obtained from (1) Pei et al. (2014) for V and ζ (Fig. 5), (2) the Iowa Environment Mesonet (IEM) database for V and IRR (IEM 2001), and (3) Wahl et al. (2015) for ζ and IRR. The details for the generation of this copula function can be found in Unnikrishnan (2015) and Unnikrishnan and Barbato (2016a). The intensity measures are directly sampled from the joint probability distribution function obtained using this copula function. The wind-surge hazard surfaces at the three locations and the wind-rainfall hazard surface (equal for all three locations) are shown in Fig. 6.

Interaction and Damage Analysis

The following quantities are adopted as interaction parameters to describe the effects of the different hazards: (1) wind pressure, p_w, for wind effects; (2) number of impacting debris, n_d, impact linear momentum, L_d, and impact kinetic energy, K_d, for windborne debris impact effects; (3) height of flood due to surge, h_f, for storm surge effects; and (4) rainfall intrusion height, h_r, for rainfall effects. The detailed procedure to calculate the interaction

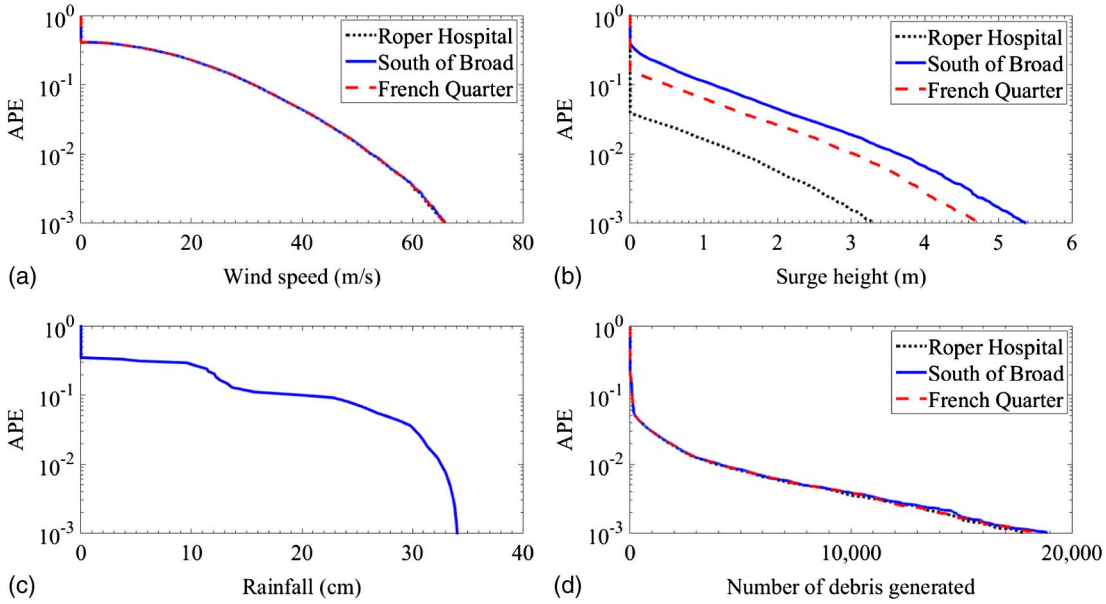

Fig. 4. Hazard curves for MDM: (a) wind; (b) surge; (c) rainfall; (d) windborne debris

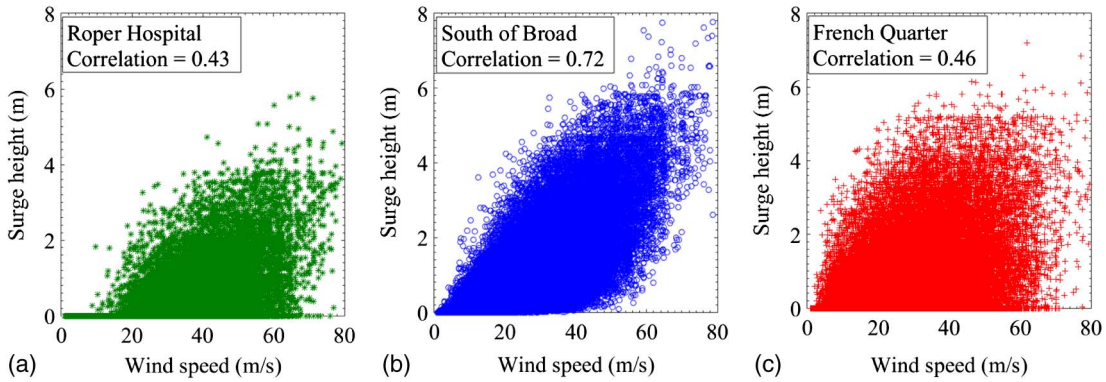

Fig. 5. Actual correlation between storm surge and wind hazard for (a) Roper Hospital; (b) South of Broad; (c) French Quarter

parameters for wind and windborne debris impact effects can be found in Unnikrishnan and Barbato (2016a). The flood height is given by

$$h_f = \zeta - h_b \tag{4}$$

where h_b = building base elevation. The rainfall intrusion height is computed as (Pita et al. 2012)

$$h_r = \frac{IRR \cdot RAF}{A_b} \cdot \left[\sum_j (d_j \cdot a_j) + a_0\right] \tag{5}$$

where RAF = rainfall admittance factor; d_j = percentage of damaged area for component j; a_j = area of component j; a_0 = area of pre-existing openings in the building; and A_b = base area of the house. The rainfall admittance factor is assumed to follow a uniform distribution ranging from 0.2 to 0.5 (Straube and Burnett 2000).

The structural analysis phase is not performed explicitly for the type of structures considered here, and the capacity of vulnerable components is directly compared to the corresponding interaction parameter (Unnikrishnan and Barbato 2016a). Table 1 shows the capacity statistics for the different components of the target building and their corresponding limit states as found in the literature (Stuckley and Carter 2001; Gurley et al. 2005; Datin et al. 2011; Masters et al. 2010).

Loss Analysis Results for Different Locations

In this study, loss analysis is performed using both global vulnerability and assembly-based vulnerability approaches for all three hazard models, providing a total of six sets of loss analysis results for each of the three locations considered. The global vulnerability approach used in Unnikrishnan and Barbato (2015, 2016b) is adopted here also. The damage states of the benchmark building are mainly governed by the performance of the building envelope (damage state of the components) and are divided into five discrete damage states, varying between 0 (no damage) and 4 (destruction). The different damage states for each of the components are described in Table 2 (Vickery et al. 2006; Womble et al. 2006; Li et al. 2012). The repair cost is then generated for the corresponding damage state according to the probability distributions given in Table 3 in terms of percentage of both building value and total content cost. It is noteworthy that the damage states for rainfall intrusion are used to calculate the losses only for the building's content.

Assembly-based vulnerability analysis for wind and windborne debris losses is adopted from Unnikrishnan and Barbato (2016a).

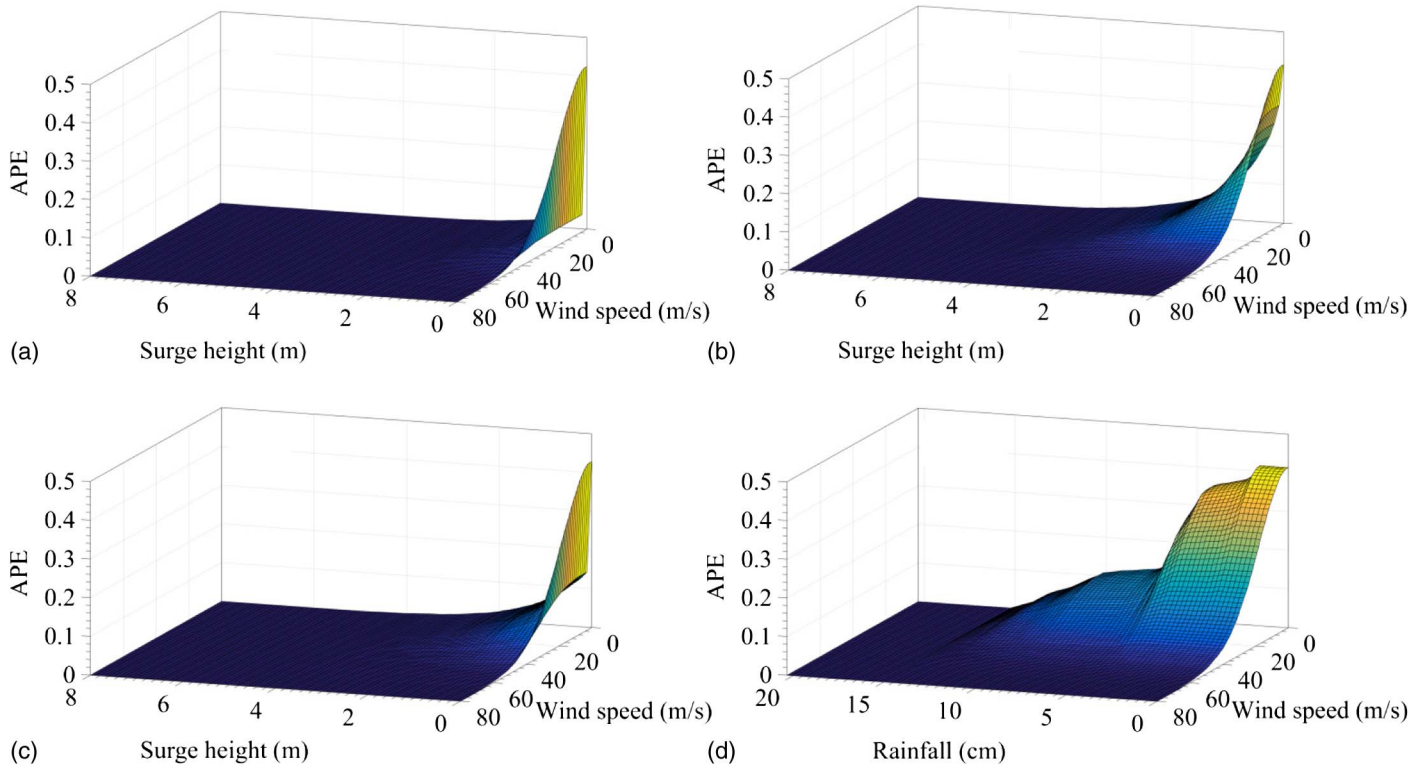

Fig. 6. Hazard surfaces obtained using JDM: (a) surge-wind for Roper Hospital; (b) surge-wind for South of Broad; (c) surge-wind for French Quarter; (d) rainfall-wind

Table 1. Statistics for Limit State Capacity of Different Benchmark Structure Components

Component	Limit state	Mean	COV	Distribution
Roof cover (shingles)	Separation or pulloff (R_{cover})	3.35 kN/m^2	0.19	Normal
Roof sheathing (nailing pattern 8d C6/12)	Separation or pulloff (R_{sh})	6.20 kN/m^2	0.12	Lognormal
Doors	Pressure failure (R_{door})	4.79 kN/m^2	0.20	Normal
Garage door	Pressure failure (R_{g_door})	3.49 kN/m^2	0.20	Normal
Windows	Pressure failure ($R_{w,pressure}$)	3.33 kN/m^2	0.20	Normal
	Impact failure ($R_{w,impact}$)	4.72 kg m/s	0.23	Lognormal
Wall sheathing	Pressure failure ($R_{wsh,pressure}$)	6.13 kN/m^2	0.40	Normal
	Impact failure ($R_{wsh,impact}$)	642.00 kg m^2/s^2	0.07	Lognormal
Roof–wall connections (wood)	Tensile failure ($R_{wcon,wood}$)	16.28 kN/panel	0.20	Lognormal
Wall (wood)	Lateral failure ($R_{wall,wl}$)	10.80 kN/panel[a] 7.06 kN/panel[b]	0.25	Normal
	Uplift failure ($R_{wall,wu}$)	9.00 kN/m[a] 5.80 kN/m[b]	0.25	Normal

[a]Toe-nail connection.
[b]Sheathing nail connection.

Table 2. Damage States for Residential Buildings

Damage state	Qualitative damage	Roof cover loss (%)	Roof deck loss	Roof failure	Wall failure	Flood height (m)	Rainfall intrusion (cm)
0	Very minor damage	≤2	No	No	No	None	$0 < h_r \le 0.02$
1	Minor damage	>2 and ≤15	No	No	No	$h_f \le 0.003$	$0.02 < h_r \le 0.25$
2	Moderate damage	>15 and ≤50	1–3 panels	No	No	$0.003 < h_f \le 0.61$	$0.25 < h_r \le 1.00$
3	Severe damage	>50	>3 panels and ≤25%	No	No	$0.61 < h_f \le 2.49$	$1.00 < h_r \le 2.50$
4	Destruction	—	>25%	Yes	Yes	$h_f > 2.49$	$h_r > 2.50$

For flood loss it is adopted from Taggart (2009), in which damage and subsequent loss to each component and to the building's content are calculated based on flood height (h_f). Assembly-based vulnerability analysis for rainfall loss is based on *HAZUS-MH*; that is, it uses empirical functions that express the content loss from individual component damage as a percentage of total content value (Unnikrishnan and Barbato 2016a). The results of the loss analysis are presented in terms

Table 3. Statistics for Repair Cost (% Building Cost/Total Content Cost) for Different Damage States (Data from Unnikrishnan and Barbato 2015, © ASCE)

Damage state	Mean (%)	COV	Distribution
0	0.2	0.2	Lognormal
1	2	0.2	Lognormal
2	10	0.2	Lognormal
3	30	0.2	Lognormal
4	70	0.2	Lognormal

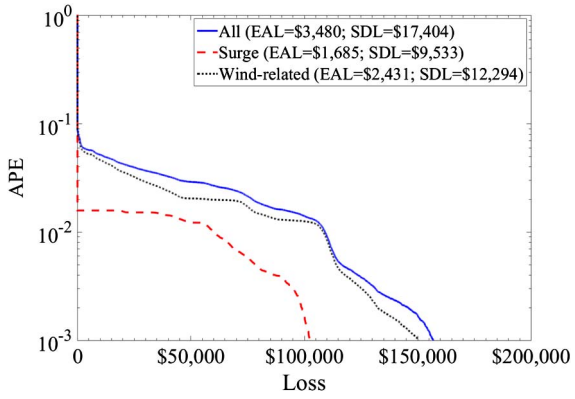

Fig. 7. Loss APEs for different hazards relative to the target building located in Roper Hospital (calculated using JDM and assembly-based vulnerability analysis)

of loss APEs, EALs, and standard deviations of annual losses (SDLs).

Loss Analysis Results for Roper Hospital

Fig. 7 plots in semilogarithmic scale the loss APEs relative to the target building at the Roper Hospital location for wind-related (i.e., wind, windborne debris, and rainfall hazards) and storm surge hazards taken independently and also for all hazards considered at the same time. These results are obtained using the JDM in conjunction with assembly-based vulnerability analysis (considered as the reference results). From Fig. 7, it is observed that the losses due to the combination of wind-related hazards are predominant when compared with the losses due to storm surge hazard. This behavior can be explained by examining the joint hazard curves for storm surge and wind hazard shown in Fig. 6(a). In particular, it is observed that wind speed values that can cause significant damage to the structure have an APE that is similar to storm surge values for which it is unlikely to have significant structural damage. It is also observed that the EAL due to the interaction of all hazards is 18.3% lower than the sum of the EALs due to the hazards taken separately, indicating a significant (negative) interaction among these hazards.

Fig. 8 plots in semilogarithmic scale the loss APEs for the target building analyzed using different combinations of vulnerability analysis and hazard models. In this case, the results obtained using global vulnerability and assembly-based vulnerability analyses are very close, with a difference in EAL for the same hazard model that ranges approximately between 0.5 and 4.5%. The EALs obtained using global vulnerability analysis are always smaller than the corresponding EALs (i.e., calculated using the same hazard model) obtained using assembly-based vulnerability analysis. It is also observed that, for the same hazard model, the loss APE curves obtained using global vulnerability analysis are very close but lower than those obtained using assembly-based vulnerability

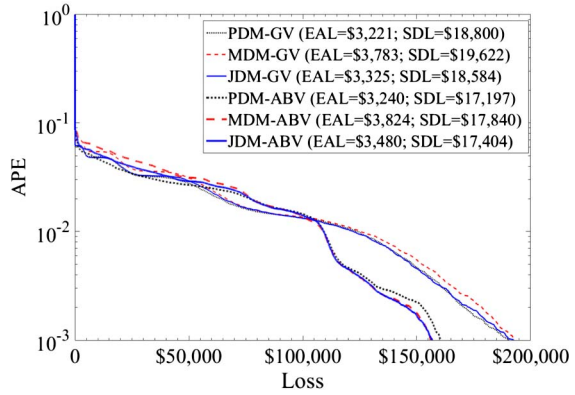

Fig. 8. Loss APEs for different hazard models and vulnerability analyses for the target building located in Roper Hospital (GV = global vulnerability; ABV = assembly-based vulnerability)

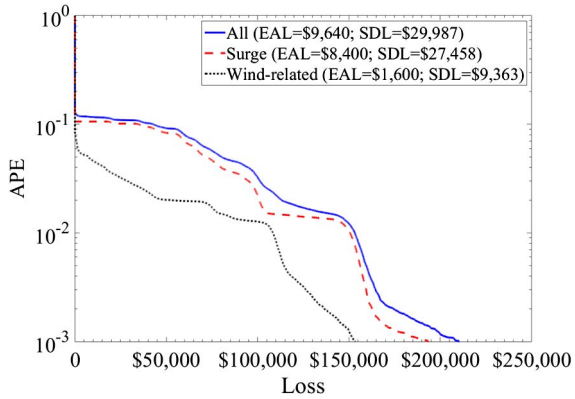

Fig. 9. Loss APEs for different hazards relative to the target building located in South of Broad (calculated using JDM and assembly-based vulnerability analysis)

analysis up to approximately $110,000, after which the global vulnerability curves become higher than the corresponding assembly-based vulnerability curves. The loss APE curves obtained using the PDM, MDM, and JDM are very close to each other when the same vulnerability analysis is used. However, the small differences for loss levels lower than approximately $110,000, which correspond to relatively high probabilities, produce differences in terms of EAL as high as 16.9% from global vulnerability analysis and 16.8% for assembly-based vulnerability analysis.

Loss Analysis Results for South of Broad

Fig. 9 plots the loss APEs (obtained using JDM in conjunction with assembly-based vulnerability analysis) relative to the target building at the South of Broad location for wind-related and storm surge hazards taken independently and for all hazards considered at the same time. These results indicate that the losses due to surge hazard are predominant when compared with the losses due to wind-related hazards. This behavior can also be explained by examining the joint hazard curves for storm surge and wind hazard shown in Fig. 6(b), from which it is observed that storm surge values that can cause significant damage have an APE that is similar to wind speed values for which it is unlikely to have significant structural damage. The EAL due to the interaction of all hazards is 3.7% lower than the sum of the EALs for the hazards taken separately, indicating a small (negative) interaction among these hazards.

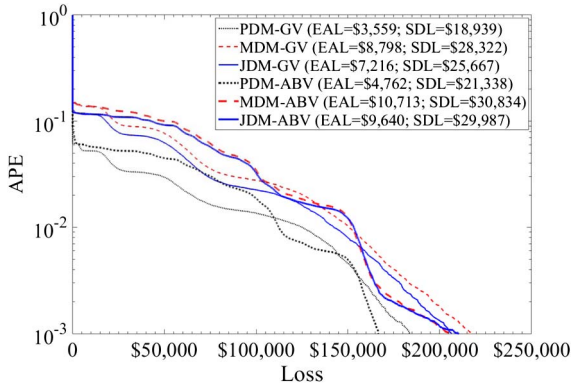

Fig. 10. Loss APEs for different hazard models and vulnerability analyses for the target building located in South of Broad (GV = global vulnerability; ABV = assembly-based vulnerability)

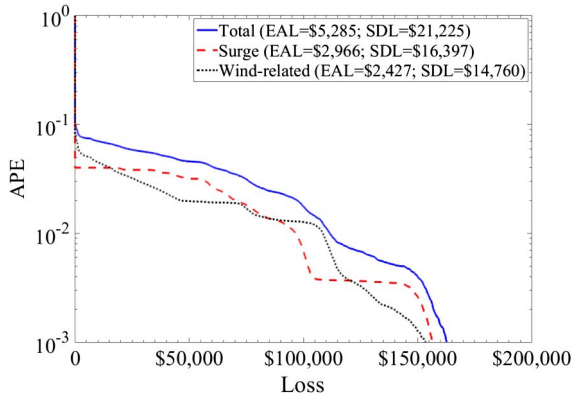

Fig. 11. Loss APEs for different hazards relative to the target building located in French Quarter (calculated using JDM and assembly-based vulnerability analysis)

Fig. 10 plots in semilogarithmic scale the loss APEs for the target building analyzed using different combinations of vulnerability analyses and hazard models. For this location, the EAL results obtained using global vulnerability and assembly-based vulnerability analyses present significant differences (25.3% for PDM, 17.9% for MDM, and 25.1% for JDM), with the global vulnerability EALs that are always lower than the corresponding assembly-based vulnerability EALs. In particular, the assembly-based vulnerability loss APE curves are higher than the corresponding global vulnerability APE curves for losses that are lower than approximately $120,000, after which the two sets of curves become very similar. When using the global vulnerability analysis, the loss APE curve obtained using the PDM is significantly lower than the curves obtained using JDM (intermediate curve) and MDM (highest curve). Similarly, when using assembly-based vulnerability analysis, the loss APE curve obtained using the PDM is significantly lower than the curves obtained using MDM and JDM. However, in this case the MDM-based curve is higher than the JDM-based curve for losses lower than approximately $70,000, and it becomes lower for losses higher than approximately $220,000. These differences result in very large variations in the estimated EALs (as large as 72.6% when using global vulnerability analysis and 61.7% when using assembly-based vulnerability analysis), with PDM that severely underestimate the EALs when compared with both MDM and JDM. Such large differences can be explained by noting that the effects on losses due to storm surge hazard are predominant when compared to the effects due to the other hazards combined. However, the PDM is not able to capture this relative importance because it underestimates storm surge height, which is modeled as a function of the wind speed.

Loss Analysis Results for French Quarter

Fig. 11 plots the loss APEs (obtained using JDM in conjunction with assembly-based vulnerability analysis) relative to the target building at the French Quarter location for wind-related and storm surge hazards taken independently and for all hazards considered at the same time. At this location, the losses due to storm surge and wind-related hazards are very close, and the EAL due to the interaction of all hazards is only 2.0% lower than the sum of the EALs due to the hazards taken separately, indicating a very small (negative) interaction among these hazards.

The loss APEs for the target building obtained using different combinations of vulnerability analyses and hazard models are shown in Fig. 12. For this location, the differences in terms of EAL estimates obtained using global vulnerability and assembly-based

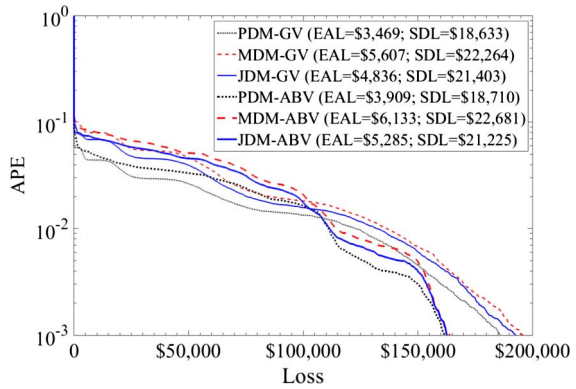

Fig. 12. Loss APEs for different hazard models and vulnerability analyses for the target building located in French Quarter (GV = global vulnerability; ABV = assembly-based vulnerability)

vulnerability analyses are 11.3% for PDM, 8.6% for MDM, and 8.5% for JDM. Also in this case the global vulnerability EALs are always lower than the corresponding assembly-based vulnerability EALs. The assembly-based vulnerability loss APE curves are higher than the corresponding global vulnerability loss APE curves for losses that are lower than approximately $110,000, after which the curves become lower. For both global vulnerability and assembly-based vulnerability analyses, PDM results in the lowest, JDM in the intermediate, and MDM in the highest curve. The variations in estimated EALs from the use of different hazard models are significant (as large as 38.1% when using global vulnerability analysis and 42.1% when using assembly-based vulnerability analysis). These differences are due to the fact that the PDM is not able to correctly estimate storm surge height and corresponding losses.

Conclusions

The study presented in this paper investigates the effects of multihazard interaction on the performance of low-rise wood-frame residential buildings subject to hurricane hazard. The multiple hazards examined here are (1) wind, (2) windborne debris, (3) storm surge, and (4) rainfall hazards, which interact during a hurricane event. The use of different hazard modeling techniques and vulnerability analyses are compared in a general PBHE framework. To the best

of the authors' knowledge, this type of investigation has not been previously attempted. Thus, a new consistent terminology to classify different hazard modeling techniques is also proposed in this paper.

A realistic case study consisting of an actual residential development in Charleston, South Carolina, is presented to establish the effects of hazard interaction in the different phases of the PBHE framework. Loss annual probabilities of exceedance expected annual losses, and annual loss standard deviations for a benchmark building are calculated for three selected locations (Roper Hospital, South of Broad, and French Quarter), using different combinations of hazard models and vulnerability techniques. Three hazard models (PDM, MDM, and JDM) and two vulnerability analyses (global vulnerability and assembly-based vulnerability) are considered, for a total of six combinations of loss analysis results for each location. For the case study considered in this paper, it is found that, when using the same hazard model and when compared with more accurate assembly-based vulnerability analysis, the global vulnerability analysis underestimates: (1) loss annual probabilities of exceedance for low loss values and (2) overall expected annual losses. It is also found that PDM can significantly underestimate expected annual losses, particularly if those due to storm surge are significant when compared with losses due to the other hazards combined.

It is significant that the consistency in loss analysis results obtained using different hazard models and vulnerability analyses strongly depends on the structural system under investigation and its location. It is evident from the results reported in this paper that the appropriate selection of both hazard model and vulnerability analysis has a significant effect on the final results of a loss analysis. Thus, whenever enough information is available, JDM for hazard analysis and assembly-based vulnerability analysis are recommended. Also, deriving general conclusions on the appropriate use of hazard and vulnerability models (particularly the simplified ones) considered in this study is a difficult task that will require a future extensive study of many structural systems and locations. This consideration should be regarded not as a limitation of the results presented in this paper but as an incentive to extend and continue the seminal work initiated in the present study in a way similar to the ongoing research performed in other, more mature performance-based engineering frameworks, such as performance-based earthquake engineering.

Acknowledgments

Partial support for this research by (1) the Longwell Family Foundation through the Fund for Innovation in Engineering Research (FIER) Program, (2) the Louisiana Board of Regents through the Economic Development Assistantship Program, (3) the Louisiana Department of Wildlife and Fisheries through Award #724534, and (4) the National Science Foundation through award CMMI #1537078 is gratefully acknowledged. The authors would also like to thank Dr. Pang from Clemson University for providing the data for joint hurricane wind and storm surge hazards for Charleston County, South Carolina. Any opinions, findings, conclusions, or recommendations expressed in this publication are those of the authors and do not necessarily reflect the views of the sponsors.

References

ASCE. (2010). "Minimum design loads for buildings and other structures." *ASCE 7-10*, Reston, VA.

Barbato, M., Petrini, F., Unnikrishnan, V. U., and Ciampoli, M. (2013). "Performance-based hurricane engineering (PBHE) framework." *Struct. Saf.*, 45, 24–35.

Batts, M. E., Cordes, M. R., Russell, L. R., Shaver, J. R., and Simiu, E. (1980). "Hurricane wind speeds in the United States." *Rep. No. BSS-124*, National Bureau of Standards, U.S. Dept. of Commerce, Washington, DC.

Beste, F., and Cermak, J. E. (1997). "Correlation of internal and area-averaged external wind pressures on low-rise buildings." *J. Wind Eng. Ind. Aerodyn.*, 69–71, 557–566.

Boon, J. D., Welch, C. S., Chen, H. S., Lukens, R. J., Fang, C. S., and Zeigler, J. M. (1978). "Storm surge height frequency analysis and model prediction for Chesapeake Bay." *Special Rep. No. 189*, Applied Marine Science and Ocean Engineering, Virginia Institute of Marine Science, Gloucester Point, VA.

Chen, C., Liu, H., and Beardsley, R. C. (2003). "An unstructured grid, finite-volume, three-dimensional, primitive equations ocean model: Application to coastal ocean and estuaries." *J. Atmos. Ocean. Technol.*, 20(1), 159–186.

Chow, C. K., and Liu, C. N. (1968). "Approximating discrete probability distributions with dependence trees." *IEEE Trans. Inform. Theory*, 14(3), 462–467.

Conner, W. C., Kraft, R. H., and Harris, D. L. (1957). "Empirical methods for forecasting the maximum storm tide due to hurricanes and other tropical storms." *Monthly Weather Rev.*, 85(4), 113–116.

Dao, T., and van de Lindt, J. (2012). "Loss analysis for wood frame buildings during hurricanes—Part I: Structure and hazard modeling." *J. Perform. Constr. Facil.*, 10.1061/(ASCE)CF.1943-5509.0000269, 729–738.

Datin, P., Prevatt, D., and Pang, W. (2011). "Wind-uplift capacity of residential wood roof-sheathing panels retrofitted with insulating foam adhesive." *J. Archit. Eng.*, 10.1061/(ASCE)AE.1943-5568.0000034, 144–154.

Der Kiureghian, A., and Liu, P. (1986). "Structural reliability under incomplete probability information." *J. Eng. Mech.*, 10.1061/(ASCE)0733-9399(1986)112:1(85), 85–104.

FEMA (Federal Emergency Management Agency). (2007). "Multi-hazard estimation methodology—Earthquake model." *Rep. No. HAZUS-MH-MR4 Technical Manual*, Dept. of Homeland Security, Washington, DC.

Georgiou, P. N. (1985). "Design wind speeds in tropical cyclone-prone regions." Ph.D. dissertation, Univ. of Western Ontario, London, ON, Canada.

Gill, J. C., and Malamud, B. D. (2014). "Reviewing and visualizing the interactions of natural hazards." *Rev. Geophys.*, 52(4), 680–722.

Gurley, K., Pinelli, J. P., Subramanian, C., Cope, A., Zhang, L., and Murphree, J. (2005). "Predicting the vulnerability of typical residential buildings to hurricane damage." Florida Public Hurricane Loss Projection Model Engineering, I.H.R. Center, Florida International Univ., Miami.

Gurley, K., Pinelli, J. P., Subramanian, C., Cope, A., Zhang, L., and Murphree, J. (2006). "Development calibration and validation of vulnerability matrices of the Florida Public Hurricane Loss Projection Model." Florida Public Hurricane Loss Projection Model Engineering, I.H.R. Center, Florida International Univ., Miami.

HAZUS-MH 2.1 [Computer software]. FEMA, Washington, DC.

Huang, Z., Rosowsky, D. V., and Sparks, P. R. (2001). "Long-term hurricane risk assessment and expected damage to residential structures." *Reliab. Eng. Syst. Saf.*, 74(3), 239–249.

IEM (Iowa Environmental Mesonet). (2001). "Iowa Environmental Mesonet database." ⟨http://www.mesonet.agron.iastate.edu/request/download.phtml?network=FL_ASOS⟩ (Apr. 16, 2014).

Irish, J. L., Resio, D. T., and Ratcliff, J. J. (2008). "The influence of storm size on hurricane surge." *J. Phys. Oceanogr.*, 38(9), 2003–2013.

Jelesnianski, C. P., Chen, J., and Shaffer, W. A. (1992). "SLOSH: Sea, lake, and overland surges from hurricanes." *NOAA Technical Rep. NWS 48*, NOAA, U.S. Dept. of Commerce, Washington, DC.

Li, Y., and Ellingwood, B. R. (2006). "Hurricane damage to residential construction in the US: Importance of uncertainty modeling in risk assessment." *Eng. Struct.*, 28(7), 1009–1018.

Li, Y., van de Lindt, J., Dao, T., Bjarnadottir, S., and Ahuja, A. (2012). "Loss analysis for combined wind and surge in hurricanes." *Nat. Hazards Rev.*, 10.1061/(ASCE)NH.1527-6996.0000058, 1–10.
Lin, N., and Vanmarcke, E. (2008). "Windborne debris risk assessment." *Prob. Eng. Mech.*, 23(4), 523–530.
Lin, N., and Vanmarcke, E. (2010). "Windborne debris risk analysis—Part I: Introduction and methodology." *Wind Struct.*, 13(2), 191–206.
Luettich, R. A., Westerink, J. J., and Scheffner, N. W. (1992). " An advanced three-dimensional circulation model for shelves, coasts, and estuaries." *Theory and methodology of ADCIRC-2DDI and ADCIRC-3DL, Technical Rep. DRP-92-6*, U.S. Army Engineer Waterways Experiment Station, Vicksburg, MS.
Masters, F. J., Gurley, K. R., Shah, N., and Fernandez, G. (2010). "The vulnerability of residential window glass to lightweight windborne debris." *Eng. Struct.*, 32(4), 911–921.
Mori, Y. (2005). "Reliability-based service life prediction and durability in structural safety assessment." Chapter 7, *Structural safety and its quality assurance*, B. R. Ellingwood and J. Kanda, eds., ASCE, Reston, VA.
Needham, H. F., and Keim, B. D. (2014). "Correlating storm surge heights with tropical cyclone winds at and before landfall." *Earth Interact.*, 18(7), 1–26.
Nelsen, R. B. (2007). *An introduction to copulas*, 2nd Ed., Springer, New York.
Nielson, B. G., and DesRoches, R. (2007). "Analytical seismic fragility curves for typical bridges in the central and southeastern United States." *Earthquake Spectra*, 23(3), 615–633.
NOAA (National Oceanic and Atmospheric Administration). (2016). "An American scientific agency focused on the conditions of the oceans and the atmosphere." ⟨http://www.ncdc.noaa.gov⟩ (Feb. 23, 2016).
NWS (National Weather Service). (2016). "An agency of the United States federal government a task of providing weather forecasts, warnings of hazardous weather, and other weather-related products to organizations and the public." http://www.nws.noaa.gov/om/coop⟩ (Feb. 23, 2016).
Pang, W., Pei, B., Testik, F., and Ravichandran, N. (2014). "Loss estimation for combined hurricane wind and surge for Charleston South Carolina." *Safety, reliability, risk and life-cycle performance of structures and infrastructures*, G. Deodatis, B. R. Ellingwood, and D. M. Frangopol, eds., CRC Press, Boca Raton, FL, 1227–1232.
Pei, B., Pang, W., Testik, F., Ravichandran, N., and Liu, F. (2014). "Mapping joint hurricane wind and surge hazards for Charleston, South Carolina." *Nat. Hazards*, 74(2), 375–403.
Phan, L. T., Simiu, E., McInerney, M. A., Taylor, A., Glahn, B., and Powell, M. D. (2007). "Methodology for development of design criteria for joint hurricane wind speed and storm surge events: Proof of concept." *NIST Technical Note 1482*, National Institute of Standards and Technology, Gaithersburg, MD.
Pietrafesa, L., Xie, L., and Dickey, D. (2002). "NCSU CEMEPS: The North Carolina state University coastal and estuary model and environmental prediction system." *Solutions to Coastal Disasters '02*, ASCE, Reston, VA, 441–455.
Pita, G., Pinelli, J. P., Cocke, S., Gurley, K., Mitrani-Reiser, J., Weekes, J., and Hamid, S. (2012). "Assessment of hurricane-induced internal damage to low-rise buildings in the Florida Public Hurricane Loss Model." *J. Wind Eng. Ind. Aerodyn.*, 104–106, 76–87.
Porter, K. A., Kiremidjian, A. S., and LeGrue, J. S. (2001). "Assembly-based vulnerability of buildings and its use in performance evaluation." *Earthquake Spectra*, 17(2), 291–312.
Powell, M. D., and Houston, S. H. (1995). "Real-time damage assessment in hurricanes." *Proc., 21st American Meteorological Society Conf. on Hurricanes and Tropical Meteorology*, American Meteorological Society, Boston, 500–502.
Rosowsky, D. V., Mudd, L., and Letchford, C. (2016). "Assessing climate change impact on the joint wind-rain hurricane hazard for the northeastern U.S. coastline." *Risk analysis of natural hazards: Interdisciplinary challenges and integrated solutions*, Springer International, Cham, Switzerland, 113–134.
Straube, J. F., and Burnett, E. F. P. (2000). "Simplified prediction of driving rain deposition." *Proc., Int. Building Physics Conf.*, FAGO, Eindhoven, Netherlands.
Stuckley, A., and Carter, R. (2001). "Perforation threshold speeds of windborne debris for various wall and above ground shelter concepts." *Internal Rep.*, Wind Engineering Research Center, Texas Tech Univ., Lubbock, TX.
Taggart, M. (2009). "Performance based design of woodframe structures for flooding." Master's thesis, Colorado State Univ., Fort Collins, CO.
Thomalla, F., Brown, J., Kelman, I., Möller, I., Spence, R., and Spencer, T. (2002). "Towards an integrated approach for coastal flood impact assessment." *Proc., Solutions to Coastal Disasters '02*, ASCE, Reston, VA, 142–158.
Thompson, E., and Cardone, V. (1996). "Practical modeling of hurricane surface wind fields." *J. Waterway Port Coastal Ocean Eng.*, 10.1061/(ASCE)0733-950X(1996)122:4(195), 195–205.
Tuleya, R. E., DeMaria, M., and Kuligowski, R. J. (2007). "Evaluation of GFDL and simple statistical model rainfall forecasts for U.S. landfalling tropical storms." *Weather Forecasting*, 22(1), 56–70.
Unnikrishnan, V., and Barbato, M. (2015). "Performance-based hurricane risk assessment of residential structures with consideration of multiple hazard." *Proc., Structures Congress 2015*, ASCE, Reston, VA, 1389–1400.
Unnikrishnan, V., and Barbato, M. (2016a). "Performance-based hurricane engineering: A multi-hazard approach." Chapter 16, *Multi-hazard approaches to civil infrastructure engineering*, P. Gardoni and J. M. LaFave, eds., Springer International, Cham, Switzerland, 337–356.
Unnikrishnan, V., and Barbato, M. (2016b). "Performance-based comparison of different storm mitigation techniques for residential buildings." *J. Struct. Eng.*, 10.1061/(ASCE)ST.1943-541X.0001469, 04016011.
Unnikrishnan, V. U. (2015). "Probabilistic performance-based hurricane engineering (PBHE) framework." Ph.D. dissertation, Louisiana State Univ. and Agricultural and Mechanical College, Baton Rouge, LA.
USACE (U.S. Army Corps of Engineers). (2000). "Generic depth-damage relationships." Washington, DC.
van de Lindt, J., and Taggart, M. (2009). "Fragility analysis methodology for performance-based analysis of wood-frame buildings for flood." *Nat. Haz. Rev.*, 10.1061/(ASCE)1527-6988(2009)10:3(113), 113–123.
Vickery, P., Lin, J., Skerlj, P., Twisdale, L., and Huang, K. (2006). "HAZUS-MH hurricane model methodology—Part I: Hurricane hazard, terrain, and wind load modeling." *Nat. Haz. Rev.*, 10.1061/(ASCE)1527-6988(2006)7:2(82), 82–93.
Vickery, P., Skerlj, P., and Twisdale, L. (2000). "Simulation of hurricane risk in the U.S. using empirical track model." *J. Struct. Eng.*, 10.1061/(ASCE)0733-9445(2000)126:10(1222), 1222–1237.
Vickery, P., and Twisdale, L. (1995). "Prediction of hurricane wind speeds in the United States." *J. Struct. Eng.*, 10.1061/(ASCE)0733-9445(1995)121:11(1691), 1691–1699.
Wahl, T., Jain, S., Bender, J., Meyers, S. D., and Luther, M. E. (2015). "Increasing risk of compound flooding from storm surge and rainfall for major US cities." *Nature Clim. Change*, 5(12), 1093–1097.
Womble, A. J., Ghosh, S., Adams, B., and Friedland, C. J. (2006). "Advanced damage detection for Hurricane Katrina: Integrating remote sensing and VIEWS$_{TM}$ field reconnaissance." *MCEER-06-SP02 Rep.*, Multidisciplinary Center for Earthquake Engineering Research, Buffalo, NY.
Zaghi, A. E., et al. (2016). "Forum paper: Establishing common nomenclature, characterizing the problem, and identifying future opportunities in multihazard design." *J. Struct. Eng.*, 10.1061/(ASCE)ST.1943-541X.0001586, H2516001.